ACS APPLIED MATERIALS & INTERFACES

www.acsami.org

Research Article

Highly Resilient Dual-Crosslinked Hydrogel Adhesives Based on a Dopamine-Modified Crosslinker

Gi-Yeon Han, Ji Yong Park, Tae-Hyung Lee, Mo-Beom Yi, and Hyun-Joong Kim*

Cite This: https://doi.org/10.1021/acsami.2c04791

Read Online

ACCESS | Metrics & More | Article Recommendations | Supporting Information

ABSTRACT: Hydrogels are promising material for wound dressing and tissue engineering. However, owing to their low tissue adhesion in a moist environment and lack of flexibility, hydrogels are still not widely applied in movable parts, such as joints. Herein, we report a dual-crosslinked hydrogel adhesive using a dopamine-modified and acrylate-terminated crosslinker, tri(ethylene glycol) diacrylate-dopamine crosslinker (TDC). The covalent crosslinking was formed by photopolymerization between acrylic acid (AA) and TDC, and the noncovalent crosslinking was formed by intermolecular dopamine−dopamine and dopamine−AA interactions. Our resultant hydrogel demonstrated strong tissue adhesion in a moist environment (approximately 71 kPa) and high mechanical resilience (approximately 94%) with immediate recovery at a 200% strain rate. Moreover, it accelerated wound healing upon dressing the wound site properly. Our study provides the potential for advanced polymer synthesis by introducing a functional crosslinking agent.

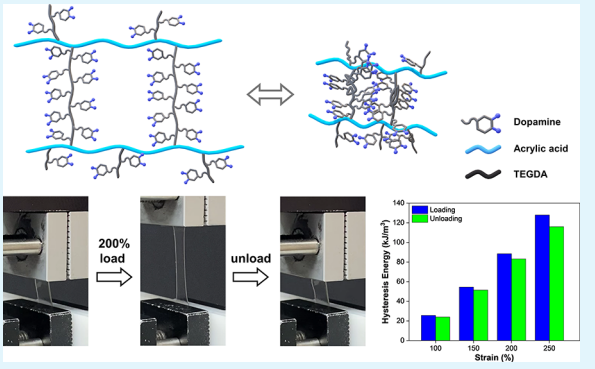

KEYWORDS: *dopamine, crosslinking agent, bioadhesives, resilience, wound healing*

INTRODUCTION

Hydrogels are three-dimensional hydrophilic polymer networks infiltrated with water.[1] Owing to their easily controllable network structure and variable functional components, hydrogels are used in various fields.[2−6] In recent years, hydrogel wound dressings have received great attention due to their high water content, similarity to biological tissues,[7] and various functionalities, such as hemostasis,[8] cell adhesion,[9] antimicrobial,[10] and anti-inflammatory[11] properties. Compared to traditional suturing and stapling, hydrogels do not need to be removed after use, thereby preventing secondary tissue damage.[12]

However, the low mechanical resilience of hydrogels limits wound dressing in movable parts, such as joints, where frequent and a large range of motion occur. To overcome this issue, a dual-crosslinked network has been proposed. Dual-crosslinked network hydrogels comprise a strong crosslink that maintains the hydrogel structure and a weak crosslink that dissipates energy.[13] The weak crosslink is composed of reversible sacrificial bonds, such as host−guest interactions,[14] hydrophobic associations,[15,16] polyampholytes,[17,18] metal−ligand coordinations,[19,20] and hydrogen bonding.[21] By introducing reversible sacrificial bonds, the hydrogel can accommodate mechanical loading and prevent crack development.[22]

Dopamine-based hydrogels have drawn considerable attention as biological adhesives.[23−25] These hydrogels can adhere to various surfaces in a moist environment[26,27] and have good cell affinity.[28] In particular, dopamine-based stretchable[29,30] and self-healable[31,32] hydrogel adhesives have been engineered based on reversible physical bonding of dopamine. However, previously reported dopamine-based hydrogel adhesives exhibit lower tissue adhesion than commercially available fibrin glue (∼20 kPa) and cyanoacrylate glue (∼60 kPa).[8,33−35] Considering the moist physiological environment, ensuring high wet tissue adhesion of hydrogel is critical.[33] Poor interface adhesion between a hydrogel and wound increases the risk of infections and delays tissue regeneration.[36]

Herein, we report a highly resilient hydrogel adhesive that can withstand a dynamic environment and accelerate wound healing. Inspired by the intermolecular interactions of dopamine, we synthesized a dopamine-modified and acrylate-terminated crosslinker, tri(ethylene glycol) diacrylate-dopamine crosslinker (TDC). We then synthesized an acrylic acid (AA)-TDC hydrogel adhesive (AA-TD hydrogel) *via* photopolymerization between AA and TDC. The TDC forms multiple crosslinks simultaneously without any additives. The covalent crosslink is formed through the photopolymerization of acrylates, and the noncovalent crosslinks are formed *via* intermolecular dopamine−dopamine and dopamine−AA in-

Received: March 17, 2022
Accepted: July 22, 2022

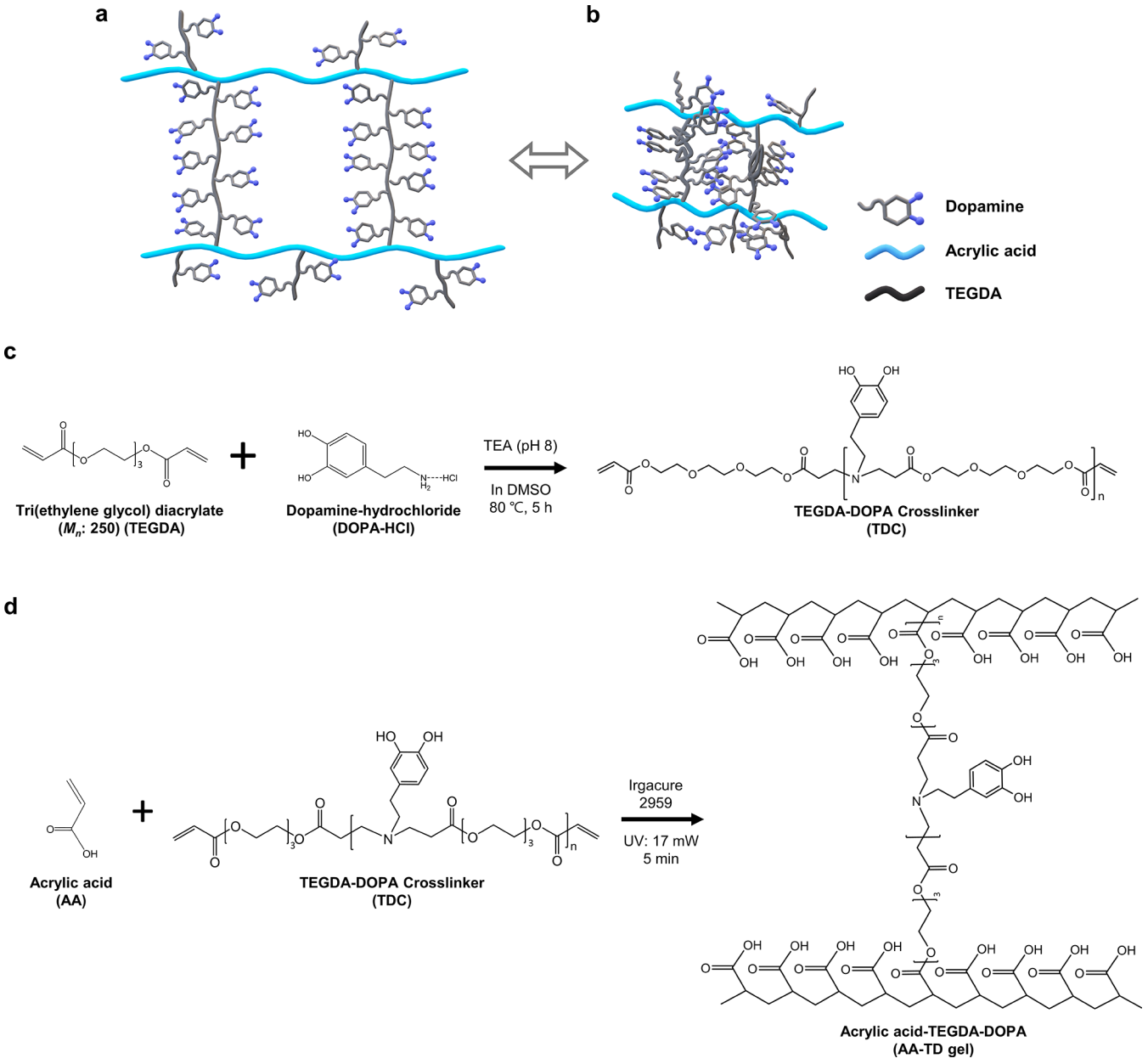

Figure 1. Schematic illustration of the AA-TD hydrogel network structure. (a) Dissociation of TDC (without intermolecular interactions) and (b) association of TDC (with intermolecular interactions). Chemical synthesis process of (c) TDC and (d) AA-TD gels.

teractions (hydrogen-bonding, $\pi-\pi$ stacking, and hydrophobic interactions) (Figure 1a,b). The AA-TD hydrogel can adhere strongly to tissues through hydrogen bonds, oxidation, and Schiff-base reaction of dopamine.[37,38] Moreover, the pH-sensitive AA backbone absorbs excess exudates and maintains a moist environment at the wound site. Our study provides an easy method to develop functional hydrogels using only a crosslinker, which can be potentially applied to electronic skins, sensors, and tissue scaffolds beyond the wound dressing materials.

RESULTS AND DISCUSSION

Preparation of Crosslinker and Hydrogel. We synthesized TDC using tri(ethylene glycol) diacrylate and dopamine hydrochloride *via* the aza-Michael reaction. The molar ratio of C═C of acrylate to NH_2 of dopamine was set at 1.1: 0.5 to make the acrylate-terminated crosslinker (Figure 1c). The Fourier transform infrared spectroscopy (FT-IR) spectrum results showed a reduction in the 810 cm^{-1} band (acrylate C═C bond), confirming that the amine group of dopamine fully reacted after 5 h (Figure S1). The molecular structure and weight of TDC were verified by ^1H NMR spectroscopy. Through 5.9−6.4 ppm proton peaks (acrylate C═C bond), we confirmed that the crosslinker was functionalized by acrylate. The molecular weight of TDC was predicted by comparing the proton peak integral values between the 5.9−6.0 ppm (acrylate C═C) and 6.55−6.75 ppm (benzene CH, next to OH). The peak integral ratio of 5.9−6.0 ppm peaks to 6.55−6.75 ppm peaks is 1−8.53, indicating that approximately 8.5 dopamine molecules are included in TDC. Hence, the average molecular weight of TDC was predicted to be approximately 3700 (Figure S2).

The hydrogel was synthesized *via* photopolymerization using AA as the base monomer and TDC as the crosslinker in

https://doi.org/10.1021/acsami.2c04791
ACS Appl. Mater. Interfaces XXXX, XXX, XXX−XXX

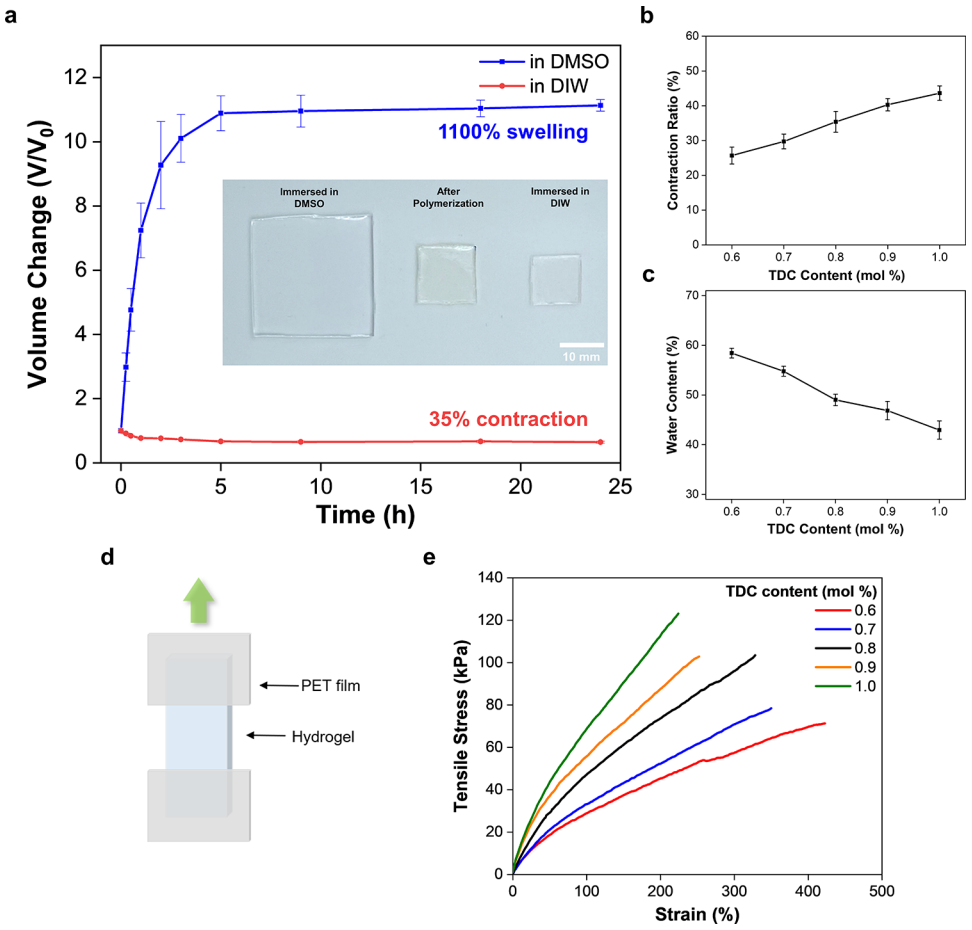

Figure 2. (a) Swelling and contraction ratio of AA-TD 0.8 gel when immersed in DMSO and DIW for 24 h, and an image of AA-TD gel at equilibrium state in each solvent. (b) Contraction ratio of AA-TD gel at equilibrium state with different TDC contents when immersed in DIW. (c) Water content of AA-TD hydrogel at equilibrium state with different TDC contents. (d) Schematic illustration of tensile test. (e) Strain–stress curve of AA-TD hydrogel with different TDC contents. The error bars represent standard deviation.

dimethyl sulfoxide (DMSO) (Figure 1d). DMSO was then removed by immersing the AA-TD gel in cold deionized water (DIW) for 10 h. The release of DMSO was monitored using ^{1}H NMR spectroscopy. 98% of DMSO was released after 1 h and DMSO was completely released after 4 h (Figure S3).

Swelling and Contraction Properties. We hypothesized that the noncovalent crosslinks would be formed by the association of TDC by intermolecular dopamine–dopamine and dopamine–AA interactions (hydrogen-bonding, π–π stacking, and hydrophobic interactions). To verify our hypothesis, we compared the change in the volume of the AA-TD 0.8 gel (0.8 mol % TDC) when immersed in DIW and DMSO for 24 h. DMSO is an organic solvent composed of polar sulfoxide and nonpolar methyl groups. Due to its amphiphilic nature, DMSO weakens intermolecular interactions.[39,40] Therefore, the effect of intermolecular interactions on the formation of noncovalent crosslinks can be verified based on the change in the volume of the AA-TD gel when immersed in each solvent. Figure 2a shows that the AA-TD gel contracted approximately up to 35% of its original volume when it was immersed in DIW. In contrast, the AA-TD gel expanded by approximately 1100% of its original volume when immersed in DMSO. In addition, the structure of the AA-TD gel was characterized using small-angle X-ray scattering (SAXS). Compared to the scattering patterns in the low-Q region (Figure S4), the AA-TD organogel (immersed in DMSO) shows a steeper slope (slope: −4.0) than the AA-TD hydrogel (immersed in DIW) (slope: −2.5). This result suggests that the domain size of AA-TD gel increased when immersed in DMSO. Through these results, we can verify the effect of intermolecular interactions on the formation of hydrogel structure. Then, to evaluate the effect of TDC contents, we measured the contraction ratio and water content of the AA-TD hydrogel in the equilibrium state with different TDC contents. As the TDC contents increased from 0.6 to 1.0%, the contraction ratio of the AA-TD hydrogel gradually increased from 25.7% (AA-TD 0.6 hydrogel) to 43.6% (AA-TD 1.0 hydrogel) (Figure 2b) and the water content decreased from 58.4% (AA-TD 0.6 hydrogel) to 42.9% (AA-TD 1.0 hydrogel) (Figure 2c). These results show that the extent of intermolecular interactions increases with the increase in TDC content, causing TDC to become more associated and the hydrogel network to become denser.

Mechanical Performances. The crosslinking density of the hydrogel greatly affects the mechanical properties of the hydrogels; therefore, we measured the changes in the mechanical properties of the hydrogel according to its TDC content using a tensile test (Figure 2d). Figure 2e shows that as the TDC content increased from 0.6 to 1.0%, the tensile strength increased by approximately 50 kPa, from 71.3 kPa (AA-TD 0.6 hydrogel) to 123.2 kPa (AA-TD 1.0 hydrogel), and fracture elongation decreased by approximately 200%,

https://doi.org/10.1021/acsami.2c04791
ACS Appl. Mater. Interfaces XXXX, XXX, XXX−XXX

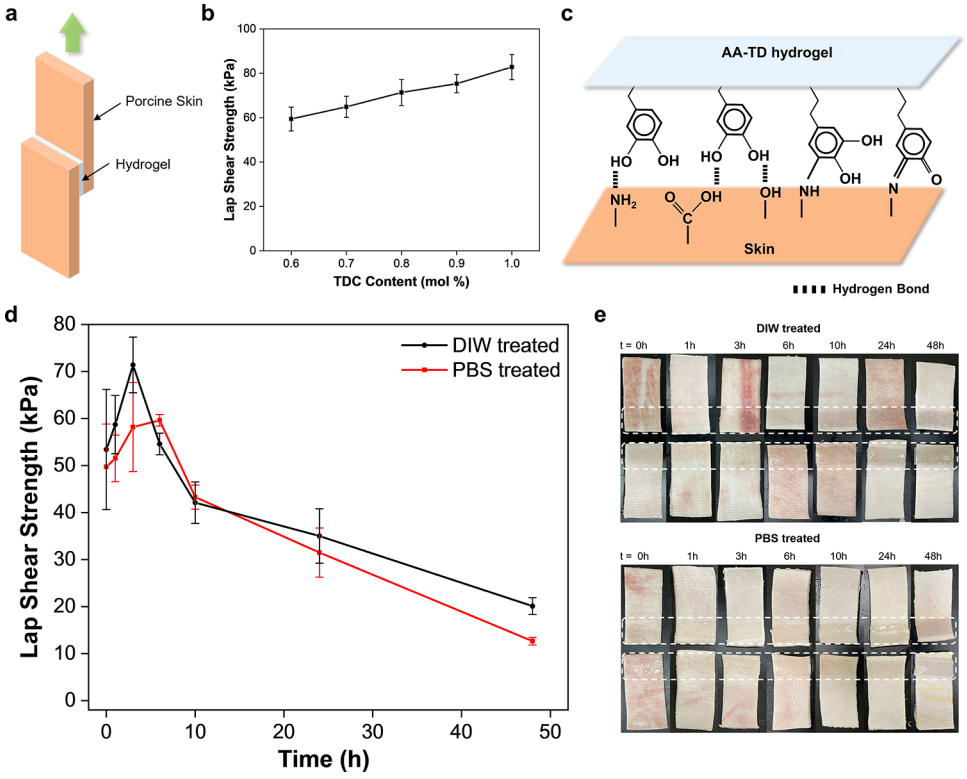

Figure 3. (a) Schematic illustration of the lap shear test. (b) Tissue adhesion strength of the AA-TD hydrogel with different TDC contents. (c) Adhesion mechanism between the skin and AA-TD hydrogel. (d) Tissue adhesion of the AA-TD 0.8 hydrogel at different time points after adhesion under DIW and phosphate-buffered saline (PBS)-treated conditions. (e) Failure mode after lap shear test and degradation profile at different time points after adhesion. The error bars represent the standard deviation.

from 422% (AA-TD 0.6 hydrogel) to 224% (AA-TD 1.0 hydrogel). A more contracted hydrogel is expected to be more elongated owing to a relatively denser network with more moieties that could be stretched more than a less dense network. However, as the crosslinking density increases, increased chain entanglement restricts the movement of the polymer chain, resulting in a decrease in elongation.

Additionally, the adhesion strength of the AA-TD hydrogel was measured with the lap shear test using porcine skin (Figure 3a and Movie S1). We selected porcine skin as the model tissue because of its high similarity to human skin.[41] Figure 3b shows that as the TDC content increases, the adhesion strength increases from 59.4 kPa (AA-TD 0.6 hydrogel) to 82.9 kPa (AA-TD 1.0 hydrogel). The AA-TD hydrogel adheres to the skin *via* hydrogen bonding, oxidation, and Schiff-base reaction between dopamine and the functional group of skins (amine, carboxylic acid, and hydroxyl groups)[42,43] (Figure 3c); therefore, as the TDC content increased, the adhesion strength increased.

In our system, the mechanical properties of the AA-TD hydrogel varied depending on the TDC content used as a crosslinker. As the TDC content increased, the tensile strength, tissue adhesion, and contraction ratio increased, whereas the fracture elongation and water content decreased. Hydrogels with 0.8 mol % TDC exhibited optimal mechanical strength (103.5 kPa tensile strength, 328% fracture elongation), tissue adhesion (71.4 kPa), and water content (48.8%). Consequently, the AA-TD 0.8 hydrogel was chosen for subsequent experiments.

Change in Hydrogel Tissue Adhesion over Time. The adhesion strength of the hydrogel must be maintained in a moist environment because the wound environment is moist due to exudate produced by damaged skin, as well as a moist physiological environment.[44] The tissue adhesion performance of hydrogel in a moist environment is a vital factor for wound dressing and greatly affects the durability of the hydrogel. Therefore, we observed the change in tissue adhesion over time (0, 1, 3, 6, 10, 24, and 48 h) under DIW- and phosphate-buffered saline (PBS) solution (pH 7.4)-treated condition (Figure 3d). The DIW-treated condition simulated a general moist environment, and the PBS-treated condition simulated a physiological condition in which body secretions were released. Both conditions were maintained by spraying DIW and PBS solutions every 12 h. For the DIW-treated condition, the maximum adhesion strength (71.4 kPa) was observed after 3 h, and for the PBS-treated condition, the maximum adhesion strength (59.6 kPa) was observed after 6 h. Over time, the adhesion strength under both conditions decreased, but the AA-TD hydrogel still exhibited excellent adhesion strength of over 30 kPa and 10 kPa after 24 and 48 h, respectively, under both conditions. When TDC is associated, the hydrophilic hydroxyl group of dopamine is exposed to the AA-TD hydrogel surface[45] and can sufficiently interact with the skin. However, as the AA-TD hydrogel absorbs water or degrades, the structure of the associated TDC is destroyed and the number of reactive sites on the hydrogel surface that interact with skin tissues decreases. In addition, the cohesion of the hydrogel decreases with its degradation, thereby decreasing the adhesion strength. The overall adhesion strength under the PBS-treated condition was lower than that under the DIW-treated condition. This is because pH-sensitive acrylic acid is used as the backbone, so the AA-TD hydrogel absorbs more

https://doi.org/10.1021/acsami.2c04791
ACS Appl. Mater. Interfaces XXXX, XXX, XXX−XXX

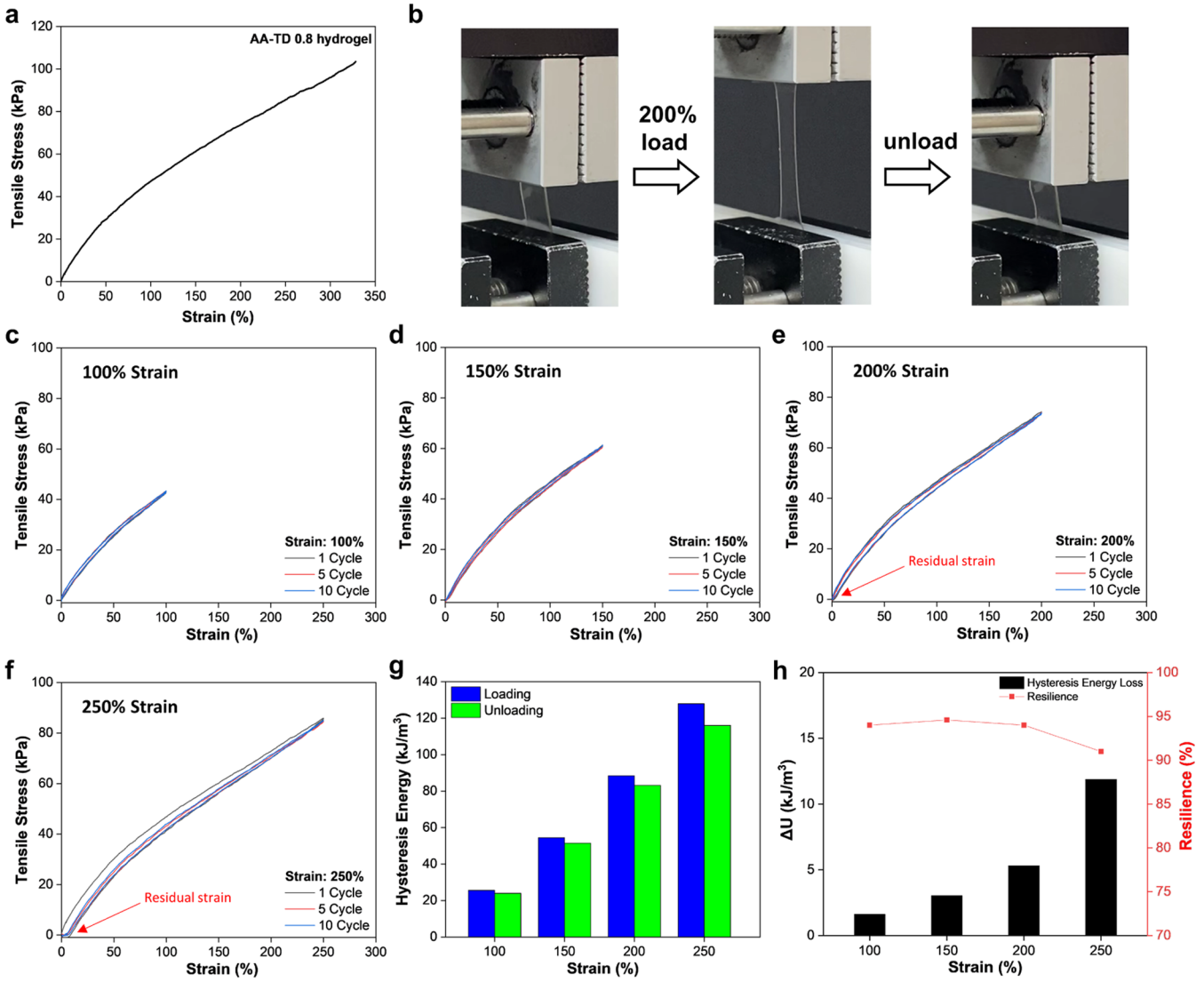

Figure 4. (a) Stress−strain curve of the AA-TD 0.8 hydrogel. (b) Image of the cyclic tensile test for the AA-TD hydrogel (strain rate: 200%). Cyclic tensile test of the AA-TD 0.8 hydrogel at (c) 100%, (d) 150%, (e) 200%, and (f) 250% strain. (g) Hysteresis energy and (h) hysteresis energy loss and resilience of the initial loading−unloading curve.

water and decomposes rapidly at higher-pH conditions.[46] However, unlike the DIW-treated condition, the maximum adhesion strength under the PBS-treated condition was measured 6 h after adhesion and exhibited a higher adhesion strength. This result is caused by an additional interaction with porcine skin due to dopamine oxidation.[47]

Recovery Performance. Movable parts, such as joints (knee, wrist, and ankle), have a frequent and large range of motion. Hence, the application of hydrogel on movable parts requires appropriate recovery properties against mechanical loading. A cyclic tensile test was conducted to evaluate the recovery properties of the AA-TD hydrogel. The residual strain, resilience, and hysteresis energy loss (ΔU) of the AA-TD hydrogel were calculated using the initial loading−unloading curves at different strain rates. At 100 and 150% strains, no residual strain was observed (Figure 4c,d), and at 200 and 250% strains, the residual strain was observed at approximately 3 and 8%, respectively (Figure 4e,f). Below 200% strain, negligible hysteresis loop changes and high resilience (approximately 94%) were observed (Movie S2). However, at 250% strain, the hysteresis energy loss increased sharply, and the resilience decreased by approximately 90% (Figure 4g,h). The AA-TD hydrogel demonstrated excellent recovery properties with high resilience and immediate recovery under 200% strain, which are mainly attributed to the reversible noncovalent crosslink. By dissipating energy through TDC dissociation, the AA-TD hydrogel can withstand large mechanical deformations[22] and returns to its original shape through TDC reassociation. However, the residual strain was observed at over 200% strain, suggesting that the fully stretched TDC can no longer dissipate energy over 200% strain. Thus, the covalent crosslinked site was destroyed.

The AA-TD hydrogel demonstrated superior mechanical performance compared to that of previously reported hydrogel adhesives for skin wound healing around joints. The AA-TD exhibit hydrogel exhibits more than 3-fold tissue adhesion (71.4 kPa) and excellent maintenance of tissue adhesion in a moist environment (over 10 kPa after 48 h),[29,48] and negligible hysteresis loop changes under a large strain rate (below 200% strain).[33,49] Moreover, the AA-TD hydrogel exhibits higher tissue adhesion than commercially available fibrin and cyanoacrylate glues.[8,33−35]

https://doi.org/10.1021/acsami.2c04791
ACS Appl. Mater. Interfaces XXXX, XXX, XXX−XXX

***In Vitro* Biocompatibility.** We evaluated the *in vitro* biodegradability and the potential toxicity of the AA-TD hydrogel. The AA-TD hydrogel is degraded under physiological conditions due to the hydrolyzable ester bond in TDC;[50] therefore, we assessed the biodegradability under physiological conditions by immersing the AA-TD hydrogel in PBS solution (pH 7.4) at 37°C. Figure 5 shows that the AA-TD hydrogel was degraded by 51% after 36 h and completely degraded after 72 h. Additionally, we evaluated the toxicity of the AA-TD hydrogel by cell viability, cell cytotoxicity, apoptosis, and live/dead assay in a hydrogel-conditioned medium. First, cell viability and cytotoxicity were measured using the WST-1 and lactate dehydrogenase (LDH) release assays over time. The effect of the hydrogel on apoptosis in STO cells was measured by Annexin V/PI staining and live/dead cell staining. Compared with the control group, the viability (Figure 6a), cytotoxicity (Figure 6b), and apoptosis (Figure 6c,d) of STO cells in the hydrogel-conditioned medium showed a nonsignificant difference, indicating that the AA-TD hydrogel is nontoxic and biocompatible.

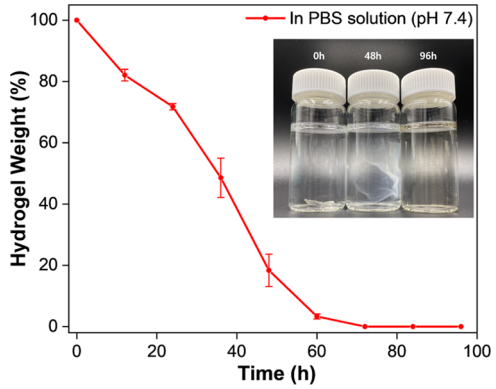

Figure 5. *In vitro* biodegradation of the AA-TD hydrogel in PBS solution (pH 7.4) for 96 h. The error bars represent the standard deviation.

Wound Healing Performance. To evaluate the wound healing performance of the AA-TD hydrogel *in vivo*, we performed quantitative (wound closure assay and vessel density) and histological analyses [hematoxylin−eosin (H&E) and Masson's trichrome staining] using a rat skin wound healing model. First, we monitored the wound size over time (0, 4, 8, and 10 days post-implantation) and observed vessel density (10 days post-implantation) in each group (control and hydrogel-treated groups). Compared to those of the control group, the AA-TD hydrogel-treated group showed a faster healing speed (Figure 7a) and increased blood vessel formation around the wound site (Figure 7b). To evaluate tissue regeneration, we compared the tissue thickness between the nonwounded (normal) and wounded (control and hydrogel-treated) groups (Figure 7c). Compared to the normal group, we observed a significant thickening of the epidermal layer in the control group, which was twice as thick as that observed in the hydrogel-treated group (Figure 7d). A thickening of the dermal layer around the wound sites was also observed, and it was thicker in the control group than in the hydrogel-treated group (Figure 7e). Moreover, the hydrogel-treated group showed a significantly higher collagen deposition (Figure 7f). Collectively, these results suggest that the AA-TD hydrogel promotes tissue regeneration[51] due to its pH-sensitive AA and high tissue adhesion in a moist environment. Excess exudates produced by wounds can be absorbed by AA, and the wound site can be protected by high tissue adhesion in a moist environment.[52] Therefore, the AA-TD hydrogel maintains a moist environment at the wound site, thereby accelerating wound healing.

CONCLUSIONS

In this study, we report a dual-crosslinked hydrogel adhesive using a dopamine-modified crosslinker. Dopamine in TDC forms a reversible noncovalent crosslink and simultaneously forms tissue adhesion. The pH-sensitive AA backbone absorbs excess exudates and maintains a moist environment at the wound site. Therefore, the AA-TD hydrogel can accelerate wound healing by protecting the wound due to high tissue adhesion and maintaining a moist environment. Our results demonstrate that the AA-TD hydrogel can be used as wound dressings in movable parts, suggesting that various functional polymers can be synthesized easily by introducing a functional crosslinker.

EXPERIMENTAL SECTION

Materials. Tri(ethylene glycol) diacrylate (TEGDA, average M_n 250) and 2-hydroxy-4′-(2-hydroxyethoxy)-2-methylpropiophenone (Irgacure 2959, 98%) were purchased from Sigma-Aldrich. Dopamine hydrochloride (99%) was purchased from Alfa Aesar. Acrylic acid (AA, 99.5%), triethylamine (TEA, 99.0%), dimethyl sulfoxide (DMSO, 99.8%), *tert*-butyl methyl ether (MTBE, 98.5%), and sodium azide (99.0%) were purchased from Samchun Chemicals Co., Ltd. 10× phosphate-buffered saline (PBS) solution was purchased from Tech & Innovation. Dulbecco's modified Eagle's medium (DMEM, #SH3243.01) was purchased from Hyclone Laboratories, Inc.

Preparation of Tri(ethylene glycol)diacrylate-Dopamine Crosslinker (TDC). TDC was synthesized *via* an aza-Michael addition reaction, as described in a previous report.[45] Dopamine hydrochloride (3.67 g, 20 mmol) and TEGDA (5.50 g, 22 mmol) were added to DMSO (21.40 g) and stirred at 25 °C until the solution became clear. TEA (1.96 g, 20 mmol) was added to adjust the pH to 8. Then, the solution was stirred at 80 °C for 5 h in the dark. After the reaction, the mixture was suction-filtered to remove TEA salt. The solution was then washed three times with MTBE to remove DMSO and the unreacted monomer. Finally, the residual solvent was removed using a rotary evaporator at 60 °C for 6 h. The yellow clear liquid was then obtained and stored at −20 °C.

Characterization of TDC (FT-IR, NMR). The reaction ratio of TDC was monitored using FT-IR spectroscopy, and the molecular structure and weight were determined using ^{1}H NMR. The IR spectra were recorded using an FT-IR spectrometer (Nicolet iS20, Thermo Fisher Scientific). ^{1}H NMR spectra were recorded using a 400-MHz NMR spectrometer (JNM-ECX400, JEOL). All ^{1}H NMR samples were measured at 25 °C in DMSO-D6, and D_2O (0.03% tetramethylsilane (δ = 0 ppm)) was used as a reference.

Preparation of Acrylic Acid-TDC (AA-TD) Hydrogel. AA-TD gel was synthesized by free-radical photopolymerization. AA (0.2 g), TDC (0.075 g, 0.8 mol % of AA), and Irgacure 2959 (0.002 g, 1 wt % of AA) were dissolved in DMSO (0.52 g, solid content was set at 35%). The mixture was then poured into a Teflon mold [12 × 75 × 0.5 mm ($W \times L \times T$)] and covered with silicon-coated PET film. The mixture was polymerized using a UV light-emitting diode lamp (intensity = 17 mW/cm^2) for 5 min. After polymerization, a yellow-transparent AA-TD gel was obtained. The AA-TD gel was immersed in DMSO for 30 min and then immersed in cold deionized water (DIW) for 10 h (fresh DIW every 1 h). White opaque AA-TD hydrogels were obtained and stored at −20 °C. Hydrogels with different crosslinker contents (0.6, 0.7, 0.9, and 1.0 mol % of TDC) were also prepared in the same way. A hydrogel with x mol % of TDC

https://doi.org/10.1021/acsami.2c04791
ACS Appl. Mater. Interfaces XXXX, XXX, XXX−XXX

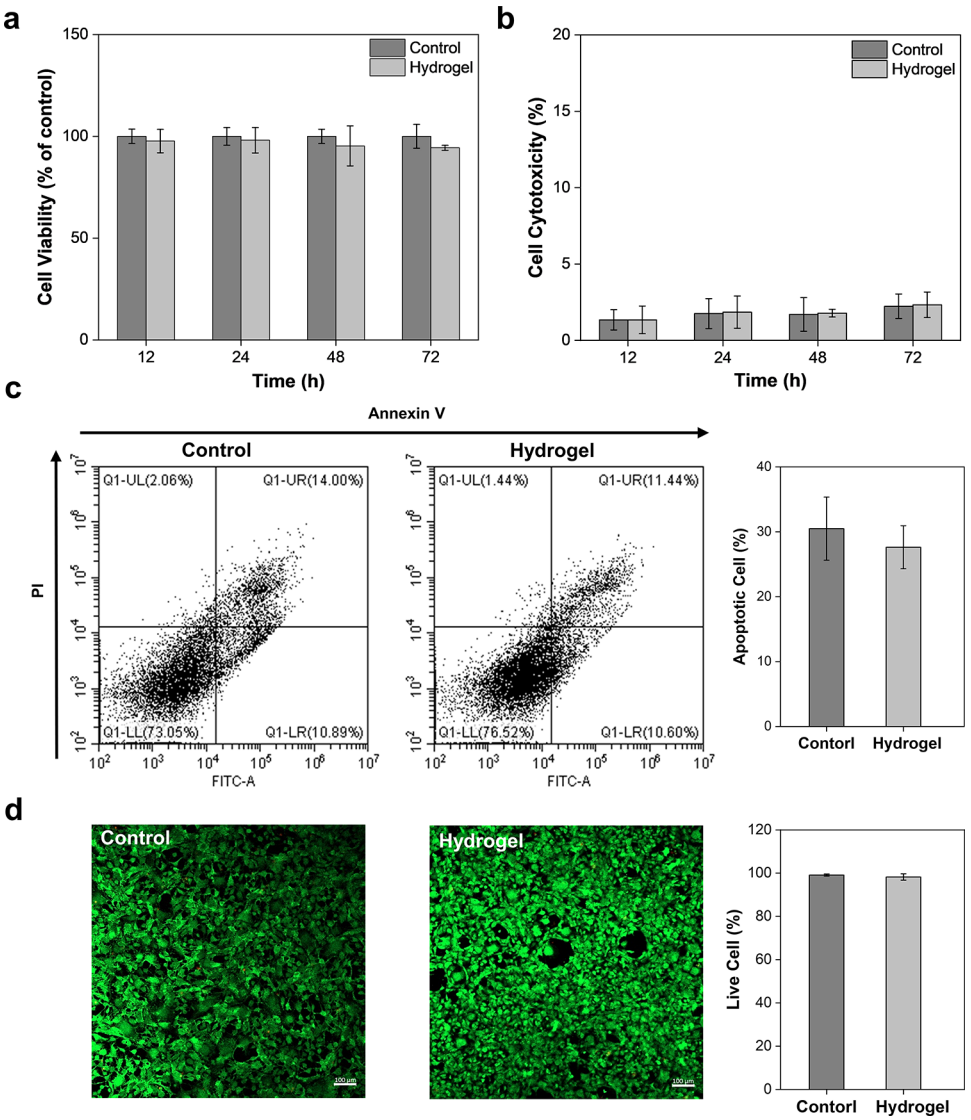

Figure 6. *In vitro* biocompatibility test of STO cells exposed to the hydrogel-conditioned medium. (a) Effect of the AA-TD hydrogel on cell viability and (b) potential toxicity of the AA-TD hydrogel over time. Effect of the AA-TD hydrogel on cell apoptosis. (c) Annexin V-FITC/PI Staining and (d) live/dead cell staining 48 h after incubation. The error bars represent the standard deviation.

was designated as the AA-TD × hydrogel. For samples without special mention, the AA-TD 0.8 hydrogel was used. The water content of the AA-TD hydrogel was calculated based on the mass loss after lyophilization.

$$\text{water content (\%)} = \frac{\text{weight of hydrogel} - \text{weight of lyophilized hydrogel}}{\text{weight of hydrogel}} \times 100 \quad (1)$$

Solvent Extraction Ratio. The release of DMSO in the AA-TD gel was measured by ^{1}H NMR. The AA-TD gel (0.1 g) was immersed in 2 mL of D_2O for 8 h (fresh D_2O every 1 h). The solvent-exchange ratio was calculated using the ^{1}H NMR integral. (D_2O_n = 4.8 ppm peak integral at n h, $DMSO_n$ = 2.5 ppm peak integral at n h)

$$\text{solvent extraction } (E_n) = \frac{DMSO_n}{D_2O_n} \quad (2)$$

$$\text{extraction ratio (\%)} = \frac{E_n}{\sum E_n} \times 100 \quad (3)$$

Swelling Ratio and Contraction Ratio. The 12 × 12 × 0.5 mm ($W \times L \times T$) AA-TD gel was immersed in DMSO and DIW at 25 °C for 24 h. The swelling and contraction ratios were calculated based on the volume change of the AA-TD gel. The initial volume of the AA-TD gel is V_o. The volume of the AA-TD gel when immersed in DMSO and DIW after n h are V_{DMSO_n} and V_{DIW_n}, respectively.

$$\text{volume change} = \frac{V_{DMSOn},\ V_{DIWn}}{V_o} \quad (4)$$

Small-Angle X-ray Scattering (SAXS). The SAXS 1D profiles were recorded using an X-ray scattering spectrometer (Xeuss 2.0, Xenocs), and Cu Kα radiation (l = 1.54056 Å) was used. The distance between the sample and the detector was 2500 mm, and the irradiation time was 1800 s. The region $0.008 < Q < 0.014$ Å^{-1} was selected to decide the slope.

Tensile and Cyclic Tensile Tests. The AA-TD hydrogel was prepared with a length of 30 mm and 10 mm grips on both ends of the hydrogel using corona-treated PET film. The tensile and cyclic tensile tests were conducted at a speed of 100 mm/min using a Texture Analyzer (TA.XT plus, Stable Micro Systems) at 25 °C and 50 ± 10% RH. The cyclic tensile test was repeated 10 times without rest. The strain rate was set at 100, 150, 200, and 250%. Residual

https://doi.org/10.1021/acsami.2c04791
ACS Appl. Mater. Interfaces XXXX, XXX, XXX−XXX

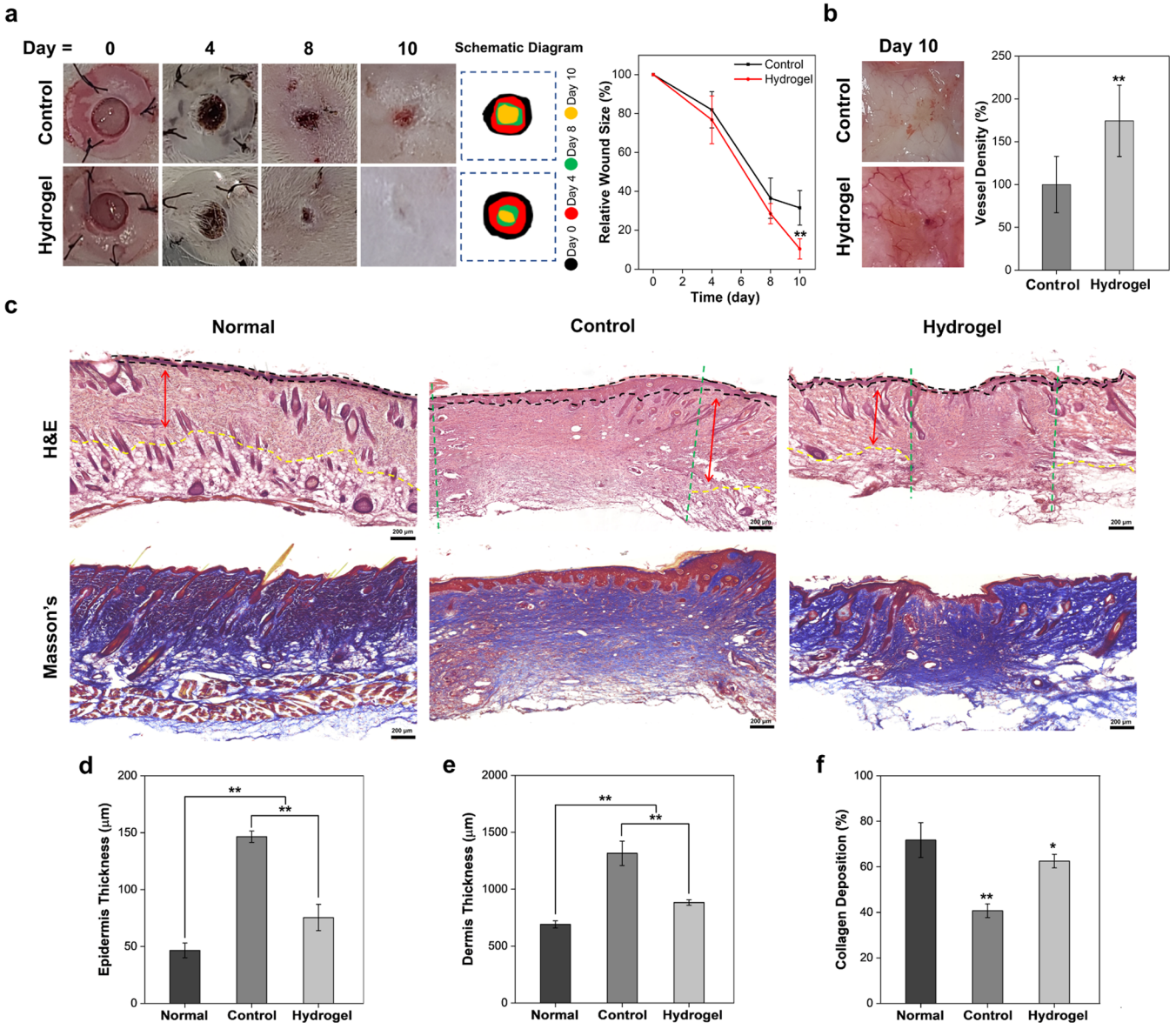

Figure 7. *In vivo* wound healing test. (a) Effect of the AA-TD hydrogel on wound healing and wound size over time. (b) Vasculogenesis around the wound site 10 days after wound healing. (c) Hematoxylin and eosin staining and Masson's trichrome staining image. Black and green dashed lines represent the boundary of the epidermis and the wound site, respectively. Red arrows represent the dermis. Comparison of (d) epidermis thickness, (e) dermis thickness, and (f) collagen deposition with the nonwounded (normal) and wounded (control and hydrogel-treated) groups. The error bars represent the standard deviation. (** $p < 0.01$, * $p < 0.05$ vs normal).

strain, hysteresis energy loss (ΔU), and resilience were calculated using the initial cycle of the loading–unloading curve.

$$\Delta U = \int_{\text{loading}} \sigma d\varepsilon - \int_{\text{unloading}} \sigma d\varepsilon \quad (5)$$

$$\text{resilience } (\%) = \frac{\int_{\text{unloading}} \sigma d\varepsilon}{\int_{\text{loading}} \sigma d\varepsilon} \times 100 \quad (6)$$

Lap Shear Test. The AA-TD hydrogel with 25 mm (L) and porcine skin with 25 × 50 mm (W × L) was used. Sodium azide solution (0.01 w/v % in DIW and 1× PBS solution) was sprayed 20 min before attaching the hydrogel to prevent degradation and dehydration of porcine skin. The AA-TD hydrogel was attached to porcine skin by applying 1 kPa pressure for 10 s and stored in a stainless tray (with cover) at 25 °C until the desired time. To maintain a moist environment, along with DIW- and PBS-treated conditions, DIW and PBS solutions were sprayed every 12 h. A lap shear test was conducted at a speed of 50 mm/min using a Texture Analyzer (TA.XT plus, Stable Micro Systems) at 25 °C and 50 ± 10% RH. The lap shear test was conducted 3 h after adhesion for samples without special mention.

***In Vitro* Biodegradation.** The lyophilized AA-TD hydrogel (40 mg) was immersed in 10 mL of 1× PBS solution (pH 7.4) at 37 °C for 4 days. At each time point, the AA-TD hydrogel was washed with DIW and lyophilized. The hydrogel weight (%) was calculated based on the mass loss of the AA-TD hydrogel.

Cell Culture. To prepare a hydrogel-conditioned medium, the lyophilized AA-TD hydrogel (0.5 mg) was immersed in 1 mL of DMEM at 37 °C for 4 days. STO cells were cultured in DMEM (10% FBS, 1% antibiotics) at 37 °C with 5% CO_2. When cells were grown to 80% confluence, the medium was then replaced with hydrogel-conditioned DMEM and incubated. Pristine DMEM was used as the control.

Cell Viability. STO cells (1×10^5 cells) were seeded into 96-well cell culture plates and cultured for 12, 24, 48, and 72 h. STO cells

https://doi.org/10.1021/acsami.2c04791
ACS Appl. Mater. Interfaces XXXX, XXX, XXX−XXX

were washed with PBS and incubated in 10% EZ-Cytox (DoGenBio) solution in 100 μL of the medium at 37 °C for 30 min. Cell viability was analyzed using a microplate spectrophotometer (Epoch 2, BioTek), and the absorbance at 450 nm was measured.

Cell Cytotoxicity. Cell cytotoxicity was evaluated by measuring the enzymatic activity of Lactate dehydrogenase (LDH) in the media. STO cells were cultured (12, 24, 48, and 72 h) and centrifuged at 600*g* for 5 min at 25 °C. The supernatant was collected, and the assay was conducted using the EZ-LDH kit according to the manufacturer's protocol. Cell cytotoxicity was analyzed using a microplate spectrophotometer (Epoch 2, BioTek), and the absorbance at 450 nm was measured.

Cell Apoptosis. STO cells (1×10^5 cells) were seeded into six-well cell culture plates and cultured for 48 h. STO cells were detached from the cell culture plates and suspended in a binding buffer. Annexin V-FITC/PI (BD Bioscience, #556547) was added and incubated for 15 min at 25 °C. Apoptotic cells were analyzed using flow cytometry (CytoFlex, Beckman Coulter).

Cell Live/Death. The cell viability of STO cells was assessed using a Live/Dead Cell Imaging Kit (Thermo Fisher Scientific, #R37601) according to the manufacturer's protocol. STO cells were seeded in μ-slide Chemotaxis 3D (IBIDI) and incubated for 48 h. After incubation, the Live Green and Dead Red reagents were mixed and added to the medium at 25 °C for 15 min. The cells were then observed using a confocal microscope system (LSM 710, Carl Zeiss).

***In Vivo* Wound Healing.** All experiments on animals were approved by the Institutional Animal Care and Use Committee of Seoul National University (SNU-210616-1-2). Six-week-old male Sprague Dawley rats were randomly divided into two groups ($n = 5$): control and hydrogel-treated groups. All rats were anesthetized with a mixture of Alfaxan (80 mg/kg) and xylazine HCl (10 mg/kg). After anesthetization, the backs of the rats were shaved and scrubbed with an organic iodine solution. A wound was made on the back skin using a 6-mm-diameter circular biopsy punch. Then, the AA-TD hydrogel was implanted in each wound and dressed with a Tegaderm film. In the control group, only the Tegaderm film was implanted. Tissue regeneration and vasculogenesis at the wound site were monitored over time (0, 4, 8, and 10 days). The wounded skin was harvested 10 days post-implantation.

Hematoxylin and Eosin (H&E) and Masson's Trichrome Staining. Tissue samples were fixed with 4% paraformaldehyde for 5 min and stained with H&E for 5 min. Samples were washed with ethanol (70, 95, and 100%) three times and then incubated in xylene for 5 min. All images were acquired using a fluorescence microscope (Eclipse Ts2, Nikon), and histological evaluations were performed blindly.

Masson's trichrome (VitroView Masson's Trichrome Stain Kit) staining was performed according to the manufacturer's protocol. All images were acquired using a fluorescence microscope (Eclipse Ts2, Nikon), and histological evaluations were performed blindly.

■ ASSOCIATED CONTENT

Supporting Information

The Supporting Information is available free of charge at https://pubs.acs.org/doi/10.1021/acsami.2c04791.

FT-IR spectrum during aza-Michael reaction of TDC; 1H NMR spectrum of TDC; solvent extraction ratio of AA-TD hydrogel; and 1D SAXS profile of AA-TD hydrogel and organogel (PDF)

Lap shear test with AA-TD hydrogel and porcine skin (Movie S1) (MOV)

Cyclic tensile test of AA-TD hydrogel at a 200% strain rate (repeated 10 times) (Movie S2) (MOV)

■ AUTHOR INFORMATION

Corresponding Author

Hyun-Joong Kim − *Program in Environmental Materials Science, Department of Agriculture, Forestry and Bioresources, Seoul National University, Seoul 08826, Republic of Korea; Research Institute of Agriculture and Life Sciences, Seoul National University, Seoul 08826, Republic of Korea;* orcid.org/0000-0002-3897-7939; Email: hjokim@snu.ac.kr

Authors

Gi-Yeon Han − *Program in Environmental Materials Science, Department of Agriculture, Forestry and Bioresources, Seoul National University, Seoul 08826, Republic of Korea;* orcid.org/0000-0002-3344-8536

Ji Yong Park − *Department of Veterinary Medicine, College of Veterinary Medicine, Seoul National University, Seoul 08826, Republic of Korea;* orcid.org/0000-0002-4486-5570

Tae-Hyung Lee − *Program in Environmental Materials Science, Department of Agriculture, Forestry and Bioresources, Seoul National University, Seoul 08826, Republic of Korea;* orcid.org/0000-0002-9112-8717

Mo-Beom Yi − *Program in Environmental Materials Science, Department of Agriculture, Forestry and Bioresources, Seoul National University, Seoul 08826, Republic of Korea;* orcid.org/0000-0002-7347-7534

Complete contact information is available at: https://pubs.acs.org/10.1021/acsami.2c04791

Author Contributions

The manuscript was written through contributions of all authors. All authors have given approval to the final version of the manuscript.

Funding

This work was supported by the Technology Innovation Program (20009198, Development and demonstration of biodegradable bioplastic prototype) funded by the Ministry of Trade, Industry & Energy (MOTIE, Korea)

Notes

The authors declare no competing financial interest.

■ REFERENCES

(1) Zhao, X.; Chen, X.; Yuk, H.; Lin, S.; Liu, X.; Parada, G. Soft Materials by Design: Unconventional Polymer Networks Give Extreme Properties. *Chem. Rev.* **2021**, *121*, 4309−4372.

(2) Griffin, D. R.; Archang, M. M.; Kuan, C. H.; Weaver, W. M.; Weinstein, J. S.; Feng, A. C.; Ruccia, A.; Sideris, E.; Ragkousis, V.; Koh, J.; Plikus, M. V.; Di Carlo, D.; Segura, T.; Scumpia, P. O. Activating an Adaptive Immune Response From a Hydrogel Scaffold Imparts Regenerative Wound Healing. *Nat. Mater.* **2021**, *20*, 560−569.

(3) Zhang, J.; Wan, L.; Gao, Y.; Fang, X.; Lu, T.; Pan, L.; Xuan, F. Highly Stretchable and Self-Healable MXene/Polyvinyl Alcohol Hydrogel Electrode for Wearable Capacitive Electronic Skin. *Adv. Electron. Mater.* **2019**, *5*, No. 1900285.

(4) Han, Z.; Wang, P.; Mao, G.; Yin, T.; Zhong, D.; Yiming, B.; Hu, X.; Jia, Z.; Nian, G.; Qu, S.; Yang, W. Dual pH-Responsive Hydrogel Actuator for Lipophilic Drug Delivery. *ACS Appl. Mater. Interfaces* **2020**, *12*, 12010−12017.

(5) Ye, T.; Wang, J.; Jiao, Y.; Li, L.; He, E.; Wang, L.; Li, Y.; Yun, Y.; Li, D.; Lu, J.; Chen, H.; Li, Q.; Li, F.; Gao, R.; Peng, H.; Zhang, Y. A Tissue-Like Soft All-Hydrogel Battery. *Adv. Mater.* **2022**, *34*, No. 2105120.

(6) Mo, J.; Dai, Y.; Zhang, C.; Zhou, Y.; Li, W.; Song, Y.; Wu, C.; Wang, Z. Design of Ultra-Stretchable, Highly Adhesive and Self-Healable Hydrogels via Tannic Acid-Enabled Dynamic Interactions. *Mater. Horiz.* **2021**, *8*, 3409−3416.
(7) Lee, K. Y.; Mooney, D. J. Hydrogels for Tissue Engineering. *Chem. Rev.* **2001**, *101*, 1869−1880.
(8) Bu, Y.; Zhang, L.; Sun, G.; Sun, F.; Liu, J.; Yang, F.; Tang, P.; Wu, D. Tetra-PEG Based Hydrogel Sealants for In Vivo Visceral Hemostasis. *Adv. Mater.* **2019**, *31*, No. 1901580.
(9) Vahedi, M.; Barzin, J.; Shokrolahi, F.; Shokrollahi, P. Self-Healing, Injectable Gelatin Hydrogels Cross-Linked by Dynamic Schiff Base Linkages Support Cell Adhesion and Sustained Release of Antibacterial Drugs. *Macromol. Mater. Eng.* **2018**, *303*, No. 1800200.
(10) GhavamiNejad, A.; Park, C. H.; Kim, C. S. In Situ Synthesis of Antimicrobial Silver Nanoparticles within Antifouling Zwitterionic Hydrogels by Catecholic Redox Chemistry for Wound Healing Application. *Biomacromolecules* **2016**, *17*, 1213−1223.
(11) Mao, X.; Cheng, R.; Zhang, H.; Bae, J.; Cheng, L.; Zhang, L.; Deng, L.; Cui, W.; Zhang, Y.; Santos, H. A.; Sun, X. Self-Healing and Injectable Hydrogel for Matching Skin Flap Regeneration. *Adv. Sci.* **2019**, *6*, No. 1801555.
(12) Han, L.; Lu, X.; Liu, K.; Wang, K.; Fang, L.; Weng, L. T.; Zhang, H.; Tang, Y.; Ren, F.; Zhao, C.; Sun, G.; Liang, R.; Li, Z. Mussel-Inspired Adhesive and Tough Hydrogel Based on Nanoclay Confined Dopamine Polymerization. *ACS Nano* **2017**, *11*, 2561−2574.
(13) Chu, W.; Nie, M.; Ke, X.; Luo, J.; Li, J. Recent Advances in Injectable Dual Crosslinking Hydrogels for Biomedical Applications. *Macromol. Biosci.* **2021**, *21*, No. e2100109.
(14) Wang, Z.; Ren, Y.; Zhu, Y.; Hao, L.; Chen, Y.; An, G.; Wu, H.; Shi, X.; Mao, C. A Rapidly Self-Healing Host-Guest Supramolecular Hydrogel with High Mechanical Strength and Excellent Biocompatibility. *Angew. Chem., Int. Ed.* **2018**, *130*, 9146−9150.
(15) Liu, X.; He, X.; Yang, B.; Lai, L.; Chen, N.; Hu, J.; Lu, Q. Dual Physically Cross-Linked Hydrogels Incorporating Hydrophobic Interactions with Promising Repairability and Ultrahigh Elongation. *Adv. Funct. Mater.* **2020**, *31*, No. 2008187.
(16) Fang, X.; Li, Y.; Li, X.; Liu, W.; Yu, X.; Yan, F.; Sun, J. Dynamic Hydrophobic Domains Enable the Fabrication of Mechanically Robust and Highly Elastic Poly(vinyl alcohol)-Based Hydrogels with Excellent Self-Healing Ability. *ACS Mater. Lett.* **2020**, *2*, 764−770.
(17) Sun, T. L.; Kurokawa, T.; Kuroda, S.; Ihsan, A. B.; Akasaki, T.; Sato, K.; Haque, M. A.; Nakajima, T.; Gong, J. P. Physical Hydrogels Composed of Polyampholytes Demonstrate High Toughness and Viscoelasticity. *Nat. Mater.* **2013**, *12*, 932−937.
(18) Huang, Y.; Xiao, L.; Zhou, J.; Liu, T.; Yan, Y.; Long, S.; Li, X. Strong Tough Polyampholyte Hydrogels via the Synergistic Effect of Ionic and Metal−Ligand Bonds. *Adv. Funct. Mater.* **2021**, *31*, No. 2103917.
(19) Liu, T.; Xie, Z.; Chen, M.; Tang, S.; Liu, Y.; Wang, J.; Zhang, R.; Wang, H.; Guo, X.; Gu, A.; Yuan, Y.; Wang, N. Mussel-Inspired Dual-Crosslinked Polyamidoxime Photothermal Hydrogel with Enhanced Mechanical Strength for Highly Efficient and Selective Uranium Extraction from Seawater. *Chem. Eng. J.* **2022**, *430*, No. 133182.
(20) Lin, P.; Ma, S.; Wang, X.; Zhou, F. Molecularly Engineered Dual-Crosslinked Hydrogel with Ultrahigh Mechanical Strength, Toughness, and Good Self-Recovery. *Adv. Mater.* **2015**, *27*, 2054−2059.
(21) Yu, H.; Rouelle, N.; Qiu, A.; Oh, J. A.; Kempaiah, D. M.; Whittle, J. D.; Aakyiir, M.; Xing, W.; Ma, J. Hydrogen Bonding-Reinforced Hydrogel Electrolyte for Flexible, Robust, and All-in-One Supercapacitor with Excellent Low-Temperature Tolerance. *ACS Appl. Mater. Interfaces* **2020**, *12*, 37977−37985.
(22) Ducrot, E.; Chen, Y.; Bulters, M.; Sijbesma, R. P.; Creton, C. Toughening Elastomers with Sacrificial Bonds and Watching Them Break. *Science* **2014**, *344*, 186−189.
(23) Zhou, D.; Li, S.; Pei, M.; Yang, H.; Gu, S.; Tao, Y.; Ye, D.; Zhou, Y.; Xu, W.; Xiao, P. Dopamine-Modified Hyaluronic Acid Hydrogel Adhesives with Fast-Forming and High Tissue Adhesion. *ACS Appl. Mater. Interfaces* **2020**, *12*, 18225−18234.
(24) Pinnaratip, R.; Bhuiyan, M. S. A.; Meyers, K.; Rajachar, R. M.; Lee, B. P. Multifunctional Biomedical Adhesives. *Adv. Healthcare Mater.* **2019**, *8*, No. 1801568.
(25) Suneetha, M.; Sun Moo, O.; Mo Choi, S.; Zo, S.; Madhusudana Rao, K.; Soo Han, S. Tissue-Adhesive, Stretchable, and Self-Healable Hydrogels Based on Carboxymethyl Cellulose-Dopamine/PEDOT:PSS via Mussel-Inspired Chemistry for Bioelectronic Applications. *Chem. Eng. J.* **2021**, *426*, No. 130847.
(26) Ye, Q.; Zhou, F.; Liu, W. Bioinspired Catecholic Chemistry for Surface Modification. *Chem. Soc. Rev.* **2011**, *40*, 4244−4258.
(27) Xie, C.; Wang, X.; He, H.; Ding, Y.; Lu, X. Mussel-Inspired Hydrogels for Self-Adhesive Bioelectronics. *Adv. Funct. Mater.* **2020**, *30*, No. 1909954.
(28) Gan, D.; Xu, T.; Xing, W.; Ge, X.; Fang, L.; Wang, K.; Ren, F.; Lu, X. Mussel-Inspired Contact-Active Antibacterial Hydrogel with High Cell Affinity, Toughness, and Recoverability. *Adv. Funct. Mater.* **2019**, *29*, No. 1805964.
(29) Yang, Z.; Huang, R.; Zheng, B.; Guo, W.; Li, C.; He, W.; Wei, Y.; Du, Y.; Wang, H.; Wu, D.; Wang, H. Highly Stretchable, Adhesive, Biocompatible, and Antibacterial Hydrogel Dressings for Wound Healing. *Adv. Sci.* **2021**, *8*, No. 2003627.
(30) Montazerian, H.; Baidya, A.; Haghniaz, R.; Davoodi, E.; Ahadian, S.; Annabi, N.; Khademhosseini, A.; Weiss, P. S. Stretchable and Bioadhesive Gelatin Methacryloyl-Based Hydrogels Enabled by in Situ Dopamine Polymerization. *ACS Appl. Mater. Interfaces* **2021**, *13*, 40290−40301.
(31) Wang, B.; Liu, J.; Niu, D.; Wu, N.; Yun, W.; Wang, W.; Zhang, K.; Li, G.; Yan, S.; Xu, G.; Yin, J. Mussel-Inspired Bisphosphonated Injectable Nanocomposite Hydrogels with Adhesive, Self-Healing, and Osteogenic Properties for Bone Regeneration. *ACS Appl. Mater. Interfaces* **2021**, *13*, 32673−32689.
(32) Deng, X.; Huang, B.; Wang, Q.; Wu, W.; Coates, P.; Sefat, F.; Lu, C.; Zhang, W.; Zhang, X. A Mussel-Inspired Antibacterial Hydrogel with High Cell Affinity, Toughness, Self-Healing, and Recycling Properties for Wound Healing. *ACS Sustainable Chem. Eng.* **2021**, *9*, 3070−3082.
(33) Chen, K.; Wu, Z.; Liu, Y.; Yuan, Y.; Liu, C. Injectable Double-Crosslinked Adhesive Hydrogels with High Mechanical Resilience and Effective Energy Dissipation for Joint Wound Treatment. *Adv. Funct. Mater.* **2021**, No. 2109687.
(34) Wu, S. J.; Yuk, H.; Wu, J.; Nabzdyk, C. S.; Zhao, X. A Multifunctional Origami Patch for Minimally Invasive Tissue Sealing. *Adv. Mater.* **2021**, *33*, No. e2007667.
(35) Zhou, L.; Dai, C.; Fan, L.; Jiang, Y.; Liu, C.; Zhou, Z.; Guan, P.; Tian, Y.; Xing, J.; Li, X.; Luo, Y.; Yu, P.; Ning, C.; Tan, G. Injectable Self-Healing Natural Biopolymer-Based Hydrogel Adhesive with Thermoresponsive Reversible Adhesion for Minimally Invasive Surgery. *Adv. Funct. Mater.* **2021**, *31*, No. 2007457.
(36) Hasani-Sadrabadi, M. M.; Sarrion, P. P. S.; Chau, Y.; Ansari, S.; Li, S. A. T.; Moshaverinia, A.; et al. An Engineered Cell-Laden Adhesive Hydrogel Promotes Craniofacial Bone Tissue Regeneration in Rats. *Sci. Transl. Med.* **2020**, *12*, No. eaay6853.
(37) Xue, B.; Gu, J.; Li, L.; Yu, W.; Yin, S.; Qin, M.; Jiang, Q.; Wang, W.; Cao, Y. Hydrogel Tapes for Fault-Tolerant Strong Wet Adhesion. *Nat. Commun.* **2021**, *12*, No. 7156.
(38) Yi, Y.; Xie, C.; Liu, J.; Zheng, Y.; Wang, J.; Lu, X. Self-Adhesive Hydrogels for Tissue Engineering. *J. Mater. Chem. B* **2021**, *9*, 8739−8767.
(39) Noack, K.; Kiefer, J.; Leipertz, A. Concentration-Dependent Hydrogen-Bonding Effects on The Dimethyl Sulfoxide Vibrational Structure in The Presence of Water, Methanol, and Ethanol. *ChemPhysChem* **2010**, *11*, 630−637.
(40) Mathis, L.; Chen, Y.; Shull, K. R. Tuning the Viscoelasticity of Hydrogen-Bonded Polymeric Materials through Solvent Composition. *Macromolcules* **2018**, *51*, 3975−3982.

https://doi.org/10.1021/acsami.2c04791
ACS Appl. Mater. Interfaces XXXX, XXX, XXX−XXX

(41) Li, J.; Celiz, A. D.; Yang, J.; Yang, Q.; Wamala, I.; Whyte, W.; Seo, B. R.; Vasilyev, N. V.; Vlassak, J. J.; Suo, Z.; Mooney, D. J. Tough Adhesives for Diverse Wet Surfaces. *Science* **2017**, *357*, 378−391.
(42) Ma, Z.; Bao, G.; Li, J. Multifaceted Design and Emerging Applications of Tissue Adhesives. *Adv. Mater.* **2021**, *33*, No. 2007663.
(43) Xu, M.; Miao, Y.; Yu, J.; Zhang, L. Physiologically-Regulated Adhesion of Hydrogels for Wound Dressing. *Adv. Mater. Interfaces* **2021**, *8*, No. 2101131.
(44) Zhang, W.; Wang, R.; Sun, Z.; Zhu, X.; Zhao, Q.; Zhang, T.; Cholewinski, A.; Yang, F. K.; Zhao, B.; Pinnaratip, R.; Forooshani, P. K.; Lee, B. P. Catechol-Functionalized Hydrogels: Biomimetic Design, Adhesion Mechanism, and Biomedical Applications. *Chem. Soc. Rev.* **2020**, *49*, 433−464.
(45) Cui, C.; Fan, C.; Wu, Y.; Xiao, M.; Wu, T.; Zhang, D.; Chen, X.; Liu, B.; Xu, Z.; Qu, B.; Liu, W. Water-Triggered Hyperbranched Polymer Universal Adhesives: From Strong Underwater Adhesion to Rapid Sealing Hemostasis. *Adv. Mater.* **2019**, *31*, No. 1905761.
(46) Karnal, P.; Jha, A.; Wen, H.; Gryska, S.; Barrios, C.; Frechette, J. Contribution of Surface Energy to pH-Dependent Underwater Adhesion of an Acrylic Pressure-Sensitive Adhesive. *Langmuir* **2019**, *35*, 5151−5161.
(47) Zhang, H.; Bre, L. P.; Zhao, T.; Zheng, Y.; Newland, B.; Wang, W. Mussel-Inspired Hyperbranched Poly(amino ester) Polymer as Strong Wet Tissue Adhesive. *Biomaterials* **2014**, *35*, 711−7119.
(48) Li, Y.; Yu, P.; Wen, J.; Sun, H.; Wang, D.; Liu, J.; Li, J.; Chu, H. Nanozyme-Based Stretchable Hydrogel of Low Hysteresis with Antibacterial and Antioxidant Dual Functions for Closely Fitting and Wound Healing in Movable Parts. *Adv. Funct. Mater.* **2021**, No. 2110720.
(49) Qu, J.; Zhao, X.; Liang, Y.; Zhang, T.; Ma, P. X.; Guo, B. Antibacterial Adhesive Injectable Hydrogels with Rapid Self-Healing, Extensibility and Compressibility as Wound Dressing for Joints Skin Wound Healing. *Biomaterials* **2018**, *183*, 185−199.
(50) Browning, M. B.; Cereceres, S. N.; Luong, P. T.; Cosgriff-Hernandez, E. M. Determination of The in Vivo Degradation Mechanism of PEGDA Hydrogels. *J. Biomed. Mater. Res. A* **2014**, *102*, 4244−4251.
(51) Loh, E. Y. X.; Mohamad, N.; Fauzi, M. B.; Ng, M. H.; Ng, S. F.; Mohd Amin, M. C. I. Development of a Bacterial Cellulose-Based Hydrogel Cell Carrier Containing Keratinocytes and Fibroblasts for Full-Thickness Wound Healing. *Sci. Rep.* **2018**, *8*, No. 2875.
(52) Korting, H. C.; Schollmann, C.; White, R. J. Management of Minor Acute Cutaneous Wounds: Importance of Wound Healing in a Moist Environment. *J. Eur. Acad. Dermatol. Venereol.* **2011**, *25*, 130−137.

https://doi.org/10.1021/acsami.2c04791
ACS Appl. Mater. Interfaces XXXX, XXX, XXX−XXX